On the Failure Behaviour of a High-Frequency Loaded CFRP-Composite

Wolfgang Förtsch[1], Horst E. Franz[1] and Klaus Friedrich[2]

[1] EADS Corporate Research Center Germany
Surface Technology and Chemical Engineering - Physical Analyses and Failure Analyses

[2] Institut für Verbundwerkstoffe GmbH, University Kaiserslautern, Germany
Materials Science

Abstract

The object of this study was to determine the fatigue behaviour of a quasi-isotropic CFRP composite under high-frequency vibration loading. The resulting decrease in stiffness is reflected by a drop in the resonance frequency. Residual-strength testing showed that there is a strong correlation between the drop in frequency and the residual strength. The course of failure was investigated at the microstructural level using microfractographic investigation. It was possible to demonstrate a relationship between the macroscopic failure and the microscopic course of failure. Thresholds were defined for the permissible fatigue load on the basis of these results.

1. INTRODUCTION AND THEORETICAL BACKGROUND

CFRP composites have been widely used in the aerospace industry as high performance materials. However, apart from their excellent properties, CFRP composites produced using standard methods have the disadvantage of very high production costs. Research during recent years has therefore been focused increasingly on producing composites using the Preform/RTM process. Up to now, it has not been possible to exploit the excellent properties of CFRP materials fully, because key questions on failure behaviour have not been satisfactorily answered. In particular, clarification has not yet been provided on the correlation between microstructure and properties in fatigue behaviour.

Although a large body of research into the fatigue behaviour of CFRP materials has already been published [1,2], this behaviour has only been determined at low frequencies between 1 and 30 Hz, mostly in the course of tension and/or compression tests [3]. It has been found that when the temperature increase during the fatigue test is small, fatigue life increases as a function of increase in load frequency. However, an increase in temperature results in a reduction of service life [4]. This research has been focused on onsets of mechanical fracture based on simple models of failure at the structural level [5].

When loads are applied under service conditions, many components are exposed to vibrations by the ambient conditions and the design of components, e.g. flaps and panels in aircraft construction. In particular, components which are exposed to sonic load or streaming are subject to loads at their natural frequencies whereby relevance comes up to the failure behaviour under these conditions. This phenomenon is generally referred to as sonic fatigue in the literature. Overall, there is limited data available relating to fatigue behaviour in the high-frequency range [6]. This is because the geometry of the test bodies under the respective vibration modes has a crucial influence on the local loads applied. The various specimen geometries are not comparable and must be examined in series of separate tests [6,7]. Hence, the tests are not suitable for determining general material properties, but are always related to specific components.

Changes in the stiffness and hysteresis of composites under fatigue load are reflected by a corresponding shift in the natural frequencies and damping. This means that a dynamic structural analysis can be used to estimate the amount of damage [8]. Failure thresholds under sonic fatigue are typically represented in diagrams with averaged stress values σ_{rms} (because of a random load) based on the number of cycles. The failure threshold determines the position of the threshold line. It is not defined clearly and is partly framed by a relatively arbitrarily fixed percentage of the drop of frequency. The type of failure to be anticipated, i.e. delaminations and fibre breakage in the upper layers, is to a large extent familiar [9].

Microfractography is the only method of verifying fatigue failure and it permits insight into fracture behaviour influenced by the microstructures of the materials at the submicroscopic level. The typical morphologies occurring on the fracture surfaces allow conclusions to be drawn on the load conditions determining failure and the formation and development of the fracture as a whole. Previous research has highlighted characteristic fracture morphologies which describe the local loading modes in each case. It is therefore possible to distinguish static as well as cyclic loaded fracture surfaces under mode I, II or mixed-mode loading. Many authors have published work in this field but we refer in particular to [10 – 13]. However, nearly all investigations were also only carried out in tests with low-frequency loads. Franz has been the only researcher to carry out microfractographic investigations on specimens which were subjected to different frequencies. Frequencies up to 92 Hz appeared to exert no influence on the formation and morphology of fatigue striations [14].
It was not possible to identify research investigating correlations between failure and material structure, the proceeding failure mechanisms and the resulting failure thresholds for the high-frequent loads. To date, the failure mechanisms leading to fibre breakage and delaminations under high frequency loads and the relevant interaction between load and failure at the microstructural level have not yet been investigated. The same is true for the influence of the general defects introduced by the RTM process.
The intention of this research is to carry out microfractographic investigations in order to trace the course of failure at the microstructural level under high frequency loads. The aim is also to describe whether certain types of dynamic loading result in specific fracture morphologies and to demonstrate any correlations that can be shown. The intention is to define threshold values for the failure using the available results and simple lifecycle diagrams. The study is also directed towards demonstrating correlations between macroscopic failure and the microscopic course of failure.

2. GEOMETRY, MATERIALS AND TESTING TECHNIQUES

A geometry needs to be found for the purpose of the investigations which is easy to record, while also reflecting real components in the form of a possible clamping geometry. Typical manufacturing defects and intrinsic structures in this geometry should be deliberately examined to ascertain their effects on composite failure.

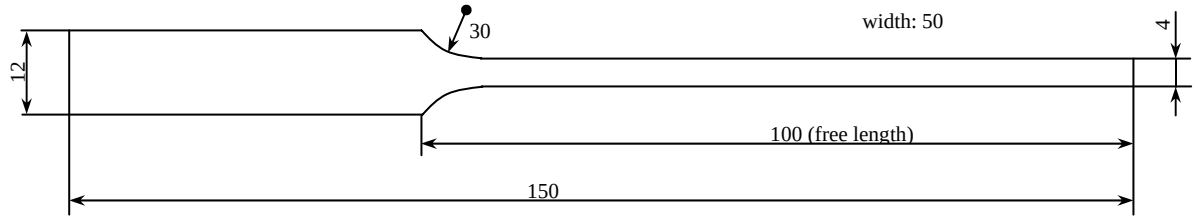

Fig.1. Geometry of the samples

The samples were defined as freely vibrating beams with a rectangular cross-section and a doubling in the clamping section (Fig. 1). The design as a bending beam rectangular in shape is easy to comprehend from a mathematical perspective and exerts minimal influence on the type of dynamic failure. Utilization of the doubling permits a reduction in the influence of the clamping forces on the vibrating sample since strain hindrance at this point would cause the elastic line to shift. The change in the cross-section of the doubling meant that the loading conditions approximated those of a real component more closely. Additional defects and lay-up malorientations were introduced which are typical at transitions like this (Fig.2).
The specimens were produced using the RTM process. A UD fabric type 863 (T800) was used as reinforcement. A single-component epoxy resin system PR 500 served as the matrix. In addition, a quasi-isotropic setup was selected: $[[00\ +45\ 90\ -45\ 00]_2]_2$.

Fig.2. Cross section of the maximum loaded area with layer waviness and resin pockets

The a×f (amplitude × frequency) - test was used to determine the fatigue strength under high-frequency load. This test involves a single-side clamped sample vibrating at its natural resonant frequency and being maintained at a constant amplitude over the whole number of cycles. The resulting maximum amplitude can be easily controlled in the experimental setup and is limited by the shaker performance. The active load during the a×f – test is chosen within the primary natural frequency of the flexible mode, where a stress ratio of R =-1 is given. It is known for this type of load that this is the most damaging loading scenario for composite materials with or without prior damage [15].
Investigations into changes in stiffness at a cycle rate of 10s involved the following parameters being recorded over the entire measuring time: the number of cycles, the momentary natural frequency, the momentary amplitude a, and the acceleration of the shaker.
In order determine the loads applied to the specimens during the a×f – test, calibration was carried out using strain gauge measurements. It was possible to show that there was good correlation between the measured strain and the mounting setup of a statically loaded beam subject to line load from one side.
The stress σ_r at the maximum loaded area can therefore be given by:

$$\sigma_r = 4 \cdot E \cdot z_0 \cdot \frac{a_{max}}{l^2} \cdot C \qquad (1)$$

where z_0 = max. margin distance, E = Young's modulus, l = free length, a_{max} = max. amplitude, and C = correction factor from the calibration (= 0,884).
In addition, the rise in temperature caused by internal friction was measured under different loading amplitudes using thermocouples laminated in the specimen. Furthermore, on-line vibrothermographic tests were conducted in order to investigate the correlation between damage and frequency and to check temperature measurement using thermocouples.
Irregularities in the reinforcement lay-up caused by manufacturing (Fig.2) meant that a shift in symmetry is caused inside the specimens. This entails the material properties becoming dependent on direction. The values of the static bending strength σ_{max} were therefore determined as minimal failure stresses of a bending semibeam clamped on one side.
Fatigue tests were carried out with CT specimens manufactured from pure resin plates with the aim of estimating the influence of the matrix system on the mechanical behaviour and the failure behaviour of the composite materials.
It was assumed that the existing temperature has substantial effects on the processes and also the energies at the crack front. The tests were therefore carried out at room temperature and 120°C (= 60% * Tg) and the crack propagation rate versus the cyclic energy release rate was determined. It was found that the intrinsic heating that occurred under load did not lead to a decrease in crack propagation within the resin, nor did the ambient temperature. There was also no essential change of the ductility of the resin over the temperature range investigated.
The specimens tested for fatigue were examined with regard to their residual tensile strength in order to estimate the extent of damage caused by the alternating load.
Microfractographic investigations were carried out using a high-resolution FE-SEM. The design of this FE-SEM makes it particularly suitable for examining plastics.

3. RESULTS AND DISCUSSION

Mechanical testing

Damage to the material appears to be due to fatigue phenomena in the a×f – test, as a function of time and applied load. The resulting change in stiffness is expressed as a change in the natural frequency. Plotting the frequency response against the number of cycles yields an in-situ observation of the course of damage over the time (Fig. 3). The nature and course of these curves depends on the material, the geometry and the load and may can be used as a criterion for estimating the damage caused.

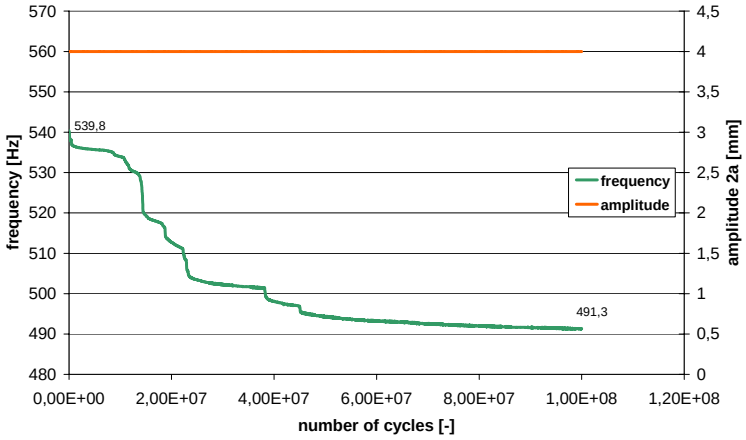

Fig.3. Typical drop in frequency plotted against the number of cycles

It appears that the drop of frequency occurs in stages, indicating an unsteady course of failure within the structure. Up to a constant load with an amplitude of 3 mm the number of cycles does not result in a decline in the natural frequency (≈ 540 Hz) of the material. The first drop in frequency is determined at an amplitude of 4 mm. This corresponds to a load of only 18% of σ_{max} with a decline in frequency of approx. 9%. The size of the drop in frequency and the shape of the curve in the form of stages are subject to a wide scatter. Nevertheless, a constant increase in frequency decline may be observed with rising load and a form of load limit value is established. At this point there is a complete breakdown in the natural frequency and ultimately component failure occurs. This limit value is established at an amplitude of 11 - 12 mm and this corresponds to a real load of approx. 50% of the minimum static failure stress.

Independently of further progression of the frequency curve, a more or less distinct drop in frequency is observed at the beginning of the test with the first loading cycles. It appears that this is caused by processes in which local stress peaks are diminished in the material. Their causes are probably to be found in defects conditional on manufacturing, for example isolated misoriented fibres.

The temperatures measured using laminated thermocouples inside the samples correspond to the results from the vibrothermographic measurements. Maximum temperatures of 120°C were measured but they do not affect failure behaviour. Specimens cooled by an airstream showed virtually no rise in internal temperature. They showed identical curve progressions for the frequency lines and identical onset of damage.

As a result of these individual tests it is possible to plot life-cycle diagrams similar to Wöhler diagrams (Fig.4). As in Wöhler diagrams, the relative maximum load σ_r/σ_{max} is plotted against the number of cycles or loading time. The life-cycle-lines are drawn in the life-cycle diagram as lines of equally decreasing frequencies in the form of logarithmic regression lines. The correlation between the decrease in frequency and the extent of damage means that the lines represent threshold lines defining the extent of the damage.

The permissible stress limit for the examined specimen geometry is between approx. 20-40% of the failure stress σ_{max} for a limiting number of load cycles of 10^8 as a function of the

respective drop in frequency. It is difficult to classify these values. If the values are considered over the number of cycles, the level of the values corresponds to the known values from alternating-load tests whilst they are, according to [4], shifted to higher numbers of load cycles. If the loading time is considered, i.e. approximately the same time that a low frequency load test (5 Hz) takes to reach a limiting number of load cycles of 10^6, the lines are almost congruent. Both scenarios would suggest viscoelastic processes at the crack tip.

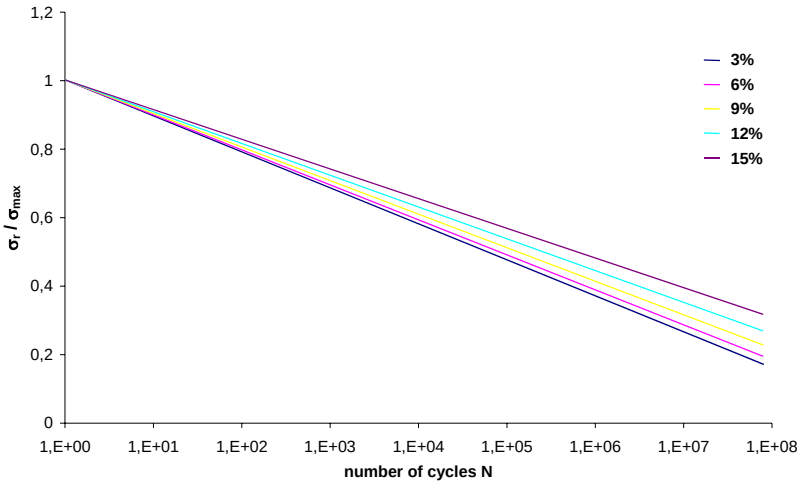

Fig.4. Lines of equally decreasing frequencies

The residual tensile strength following fatigue load was measured in a tensile test (Fig.5). The low number of samples means that it is not possible to establish an unambiguous linear correlation between the residual tensile strength and the decline in frequency. However, there appears to be a very strong decline in the values down to approx. 30% of the static tensile strength of the undamaged specimen.

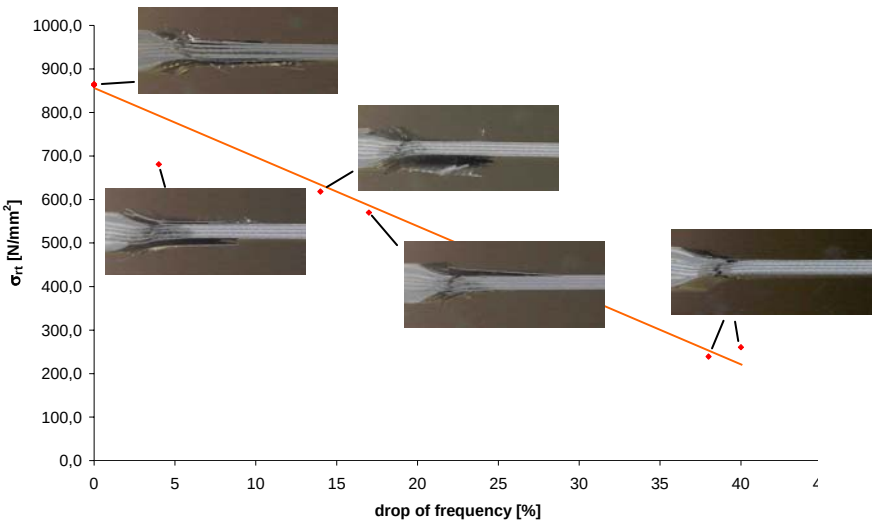

Fig.5. Strength after fatigue loading as a function of fracture

The high loss of strength already evident with a low drop in natural frequency indicates that very substantial damage occurs locally in the material. This can also be seen with the varied occurrence of fractures following failure in the tensile test. As the fall in frequency increases accompanied by a greater local weakening of the material, the length of the delaminations

decreases along the test axis. Delaminations are usually caused by transverse forces acting under tensile load. However, they cannot appear with increased weakening of the cross section in the area of the doubling.

Microfractographic investigations

Microfractographic investigations involved examination of specimens which showed a characteristic drop in frequency during the axf test. Thermographic scans showed an increase in the amount of damage as the value of the frequency decline increased in the area of the radius. No dependence between the damage of the designated top / bottom side was identified. The extent of distinct damage increases as a function of the defects. In the case of similar falls in frequency, the extent of damage identified is also similar in size.

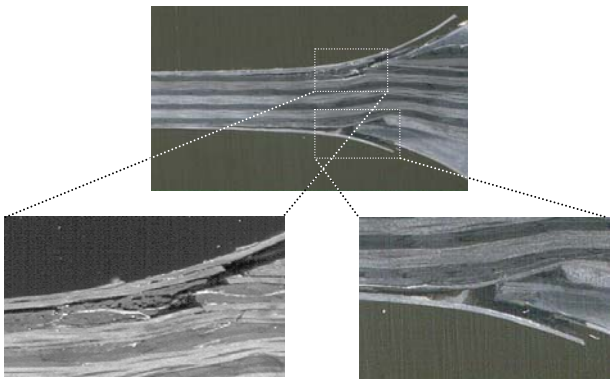

Fig.6. Cross section of the failed region (24% drop in frequency)

The micrographs showed that the main damage took place in the area of the resin pocket and the directly adjacent layers. A sample with only a 9% drop in frequency showed two cracks aligned vertically along the direction of load in the resin pocket and a delamination failure only in the directly abutting fabric layers (Fig 7). Also a specimen subject to high load (Fig. 6) evinces cracks transverse to the direction of load in the resin pocket. However, in addition to delaminations at the outer layers, there are separations of the resin pocket from its surroundings. Complete delamination of the outer layers may occur through to translaminar failure, i.e. complete fracture of the laminated fibre bundles. The resin pocket is completely rubbed off, in the same way as the opposing structure subject to the maximum load, where the upper 0° layer is delaminated without translaminar failure, whereas the ±45° and 0° layer beneath are destroyed locally.

It was possible to identify hitherto unknown fracture phenomena on the fracture surfaces of all the samples examined. However, these do not change as a function of the size of the high frequency load in any meaningful way. The fracture phenomena should therefore be represented by way of example on one characteristic fracture surface.

Fig. 7 shows a side view of the fracture surface of a specimen with 9% drop in frequency. The arched fronts where the primary front of fatigue crack propagation is blunted are clearly visible in the direction of the beam. The cracks running in the resin pocket and their continued propagation in the material are also clearly visible. These cracks may show some major disruptions of the resin due to crack branching. Points in the picture were marked with numbers to show characteristic features in the microfractographic tests. Alternatively, they were investigated with a view to understanding the chronological progress of the failure.

The fracture phenomena described in this section are characteristic for the components subject to load at high frequency and are virtually unknown in the literature. They are therefore initially described on the basis of familiar micromorphologic details and purely from the perspective of their occurrence.

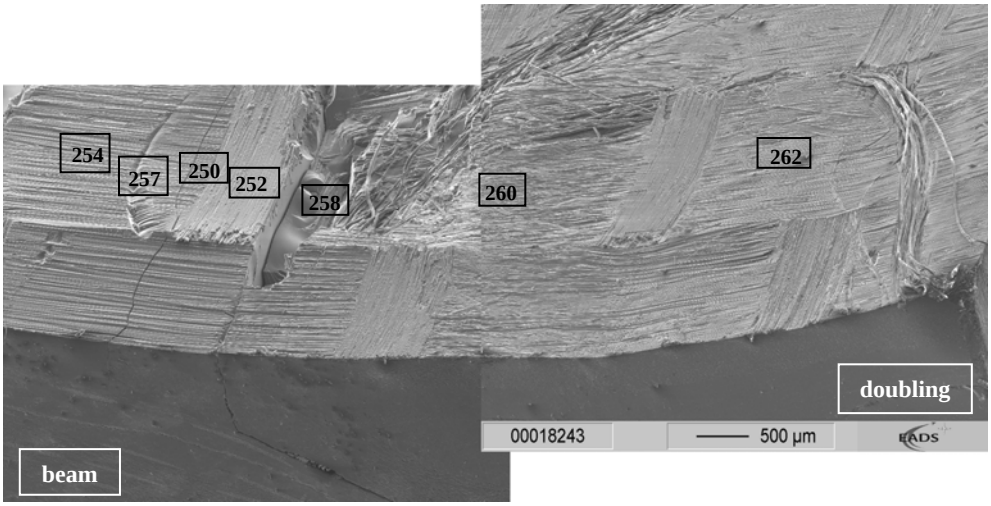

Fig.7. SEM image of a fracture surface for a sample with 9% drop in frequency

The transition of the fatigue area into the static preparation fracture (254) takes place abruptly in the form of an arched pit in the pure resin, where one flank has statically broken and the other flank demonstrates scaly structures (257). These can be recognized at higher magnification as separate characteristic features with blurred demarcations with the neighbouring ones (Fig. 8).

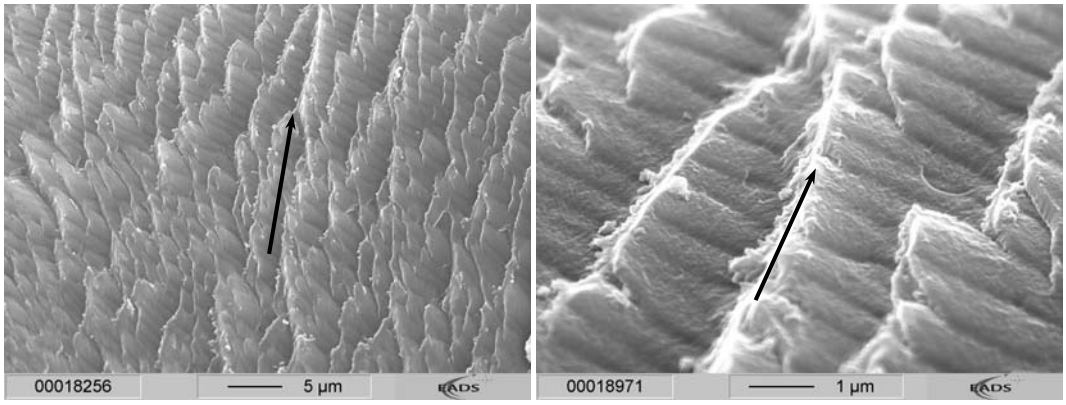

Fig.8. Fatigue striations on a scaly area (257), tilt angle: 45° (The arrow indicates the fracture direction)

When they are lined up, they are on separate planes perpendicular to the fracture direction. The corresponding structures can be seen on the matching fracture surface. Crack propagation appears here at different fracture planes which run in the direction of fracture and propagate into each other in scarp formations. The blurred demarcations of the scaly structure stand out as a wavy form and represent probably the cyclic component of the fracture morphology as fatigue striations. This would present an unambiguous proof of fatigue failure in this area.
Fatigue failure under predominant mode I component appears to be present in the whole area. This may also be expressed as typical scarps on the fracture surface and the local fracture direction can be determined from them. If the specimen is tilted a sharp angle, the fatigue striations overlaying the whole structure may be seen (Fig. 8, right).
Quite different fracture characteristics may be found in area 250 between the two transverse cracks in the resin pocket where the local fibre orientation runs parallel to the load direction.
Radiating out from the fibre beds, the fracture phenomena have a lamellar structure which partly reunites at the top and forms a closed surface (Fig 9, left). No imprints of the fibre surfaces are to be found in the fibre beds. A corresponding facture structure can be seen on the matching fracture surface (Fig. 9, right). The fibres are completely coated in resin and are

simultaneously fixed by the lamellar structure. By comparing fracture surfaces and matching fracture surfaces, it may be seen that pure matrix failure is present as a cohesive fracture of the resin, i.e. no interface failure takes place.

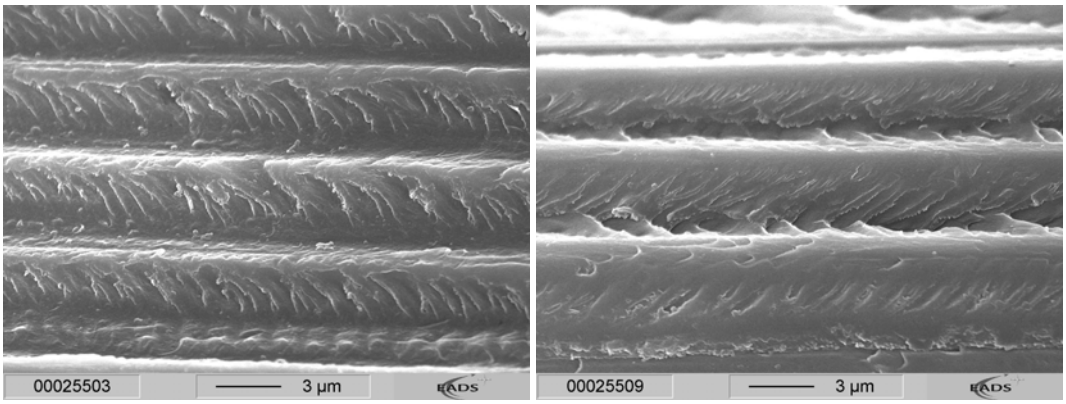

Fig.9. Fracture surface and matching fracture surface in area 250, tilt angle: 45°

Familiar fracture attributes inevitably entail a comparison with the known hackles as a characteristic phenomenon of a mode II statically loaded fracture surface. Fracture planes and shape are similar, but the purely adhesive failure points towards changed loading conditions, as they are evident from the axf test. However, in a comparison with a static lab fracture these structures cannot be found. Their occurrence indicates that they can probably be assigned to a mixed-mode failure under predominant mode II component.

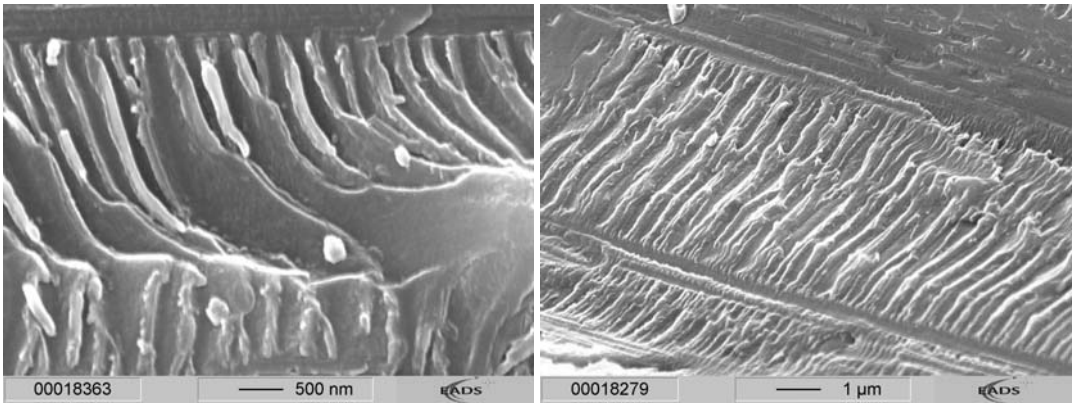

Fig.10. Left: Fracture morphology in (258), Right: Area between fibre imprints in (260)

The fracture characteristics found in the base of the resin pocket (area 258) correspond to the features in 250. The lamellar structure is more distinct, although this may be caused by a bigger fibre distance prevailing locally. Interface failure also takes place along the fibres. The magnification (Fig. 10, left) shows that the cracks were initiated in each case along the fibres being propagated into the inter-fibre areas.

No signs of fatigue crack growth are to be found in the flanks of the transverse crack and the disruption in the resin pocket. Instead, all the signs of a static fracture are found.

The occurrence of characteristic fracture features is different in the areas 260 and 262 between the resin pocket and clamping. The area near the resin pocket shows an essentially less distinct structure formation (Fig. 10, right). This suggests a comparison with mode II fatigue fracture loaded at low frequency. The occurrence of the morphology in the inter-fibre areas resembles a fracture surface after roller formation, although these are not to be found.

A much more distinct shape for the fracture characteristics is found in the area 262. The fibre direction also corresponds here to the macroscopic fracture direction, although the fracture

runs in the interface between fibres and matrix. At higher magnifications it may be seen that interface failure appears with the local fracture direction in the inter-fibre areas lying perpendicular to the macroscopic fracture direction (Fig. 11). In the further course of the emerging fracture planes, it may be seen that these fracture planes tend to be oriented in the direction of the primary crack front according to a static fracture under mixed-mode conditions.

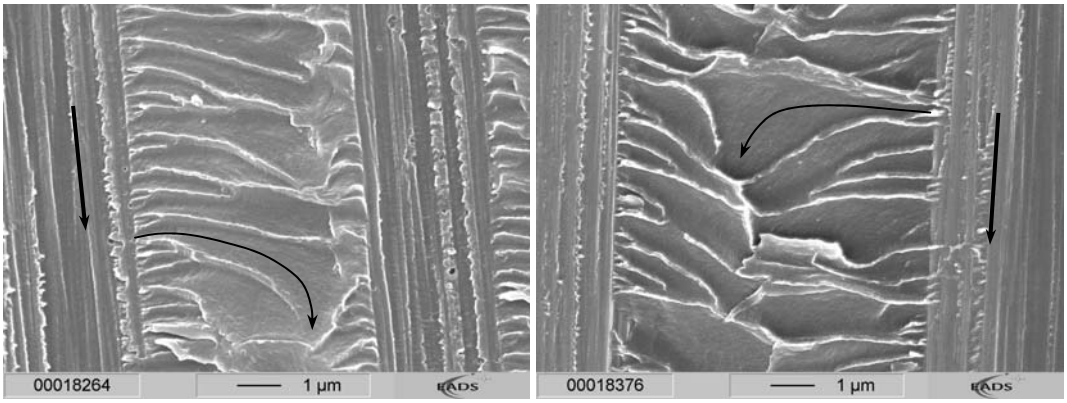

Fig.11. Fracture surface and matching fracture surface in 262 (The arrow indicates the fracture direction)

The chronological course of failure may be interpreted as a result of known fracture phenomena using microfractographic examinations of specimens subject to loads at low frequency. By contrast, fracture characteristics presented above have not been adequately described to date. Nevertheless, the intention was to understand the chronological course of failure in the component based on conclusive correlations.
When loading commences, static mode I transverse cracks appear in the resin pocket (Fig. 12). This exerts an effect later as initiation sites for fatigue crack propagation. These cracks propagate further primarily under predominant mode II load in the direction of clamping within the outer layers along the line of maximum load. Decelerated crack growth takes place in the direction of the beam. A change in the loading mode takes place in both directions, starting initially with nearly pure mode II load moving to a predominant mode I load by the end of crack propagation. If progressive damage occurs or the load is increased, the stress field and crack propagation are also shifted within the material. Additional damage propagation means that the bearing cross-section decreases in size and the supporting matrix structure is increasingly destroyed, since total failure occurs in the form of a complete frequency breakdown.

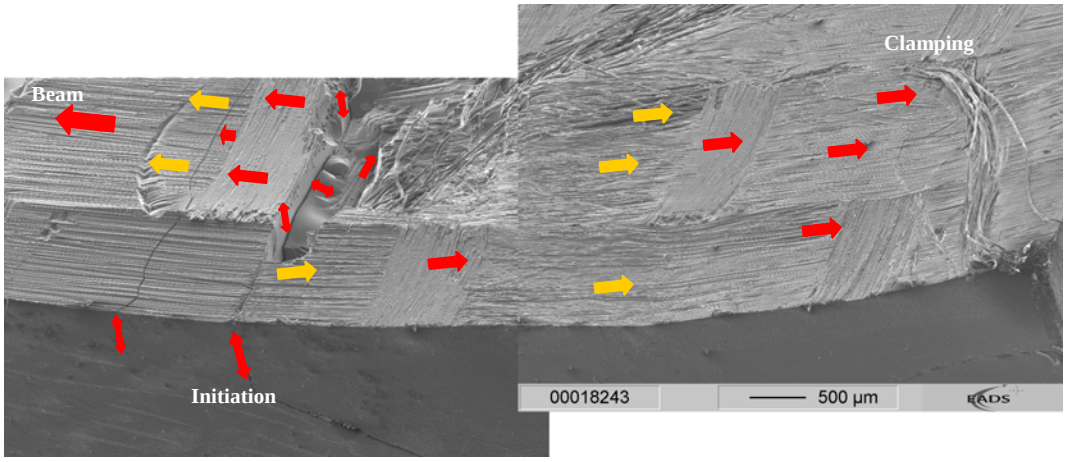

Fig.12. Course of fracture on the fracture surface (yellow: fatigue fracture, red: static fracture)

The lack of homogeneity in the construction of fibre reinforced material means that different effects interact throughout the failure and this leads to gradual failure of the material:

- The field of tension inside the sample varies due to lack of homogeneity. This leads to simultaneous crack growth at different areas.
- The growing failure itself changes the stress field and leads to an increasing stress value caused by a decrease in the residual cross-section.
- Simultaneously, crack growth is stopped locally, because energy is dissipated by the formation of new surfaces.

In the case of the a×f-test, there is a gradient of tension along the free vibrating length of the sample. This means there is a point of maximum load and fatigue in a small area next to the radius. Local failure next to the radius may be regarded as the decrease in the clamping strength of a bending beam clamped on one side.

It is possible to visualize in the form of a model the area next to the doubling radius as a flat spiral spring with a decreasing spring constant caused by the damage growth. The local damage caused by the point of maximum stress, means that the description of a common decreasing elasticity of the specimen in the a×f-test is not correct.

This makes it possible to explain the strong correlation between decrease in frequency and residual strength. The cross-section at the radius will be severely damaged locally and shows a small drop in frequency under minor loads. This means that the residual strength decreases significantly. Due to its dependence on local damage events, the residual strength is substantially determined by the local discontinuities. The residual strength could be improved by minimizing these crack initiation points.

4. CONCLUSIONS

- The curve progressions of natural frequencies plotted enable us to draw conclusions on the failure behaviour of the material. A lack of homogeneity in the construction of fibre reinforced materials means that different effects interact throughout the failure, and this leads to a gradual failure of the material.
- Fatigue tests on the matrix material and comparison of measurements with cooled specimens meant that it was not possible to provide proof of any influence by the temperature on fatigue failure, as long as loads are applied at high frequency for the designated test configuration, geometry and material design.
- Classification of the threshold lines found in the life cycle diagrams is difficult. However, if their position is considered in correlation with tests carried out with loading at low frequency, viscoelastic processes at the crack tip are probably indicated.
- This was the first time that microfractographic methods were used in investigations carried out into the failure behaviour of CFRP components subject to loads at high frequency.
- Inhomogeneities that can scarcely be avoided in RTM materials exert an effect as crack initiation sites. They can also influence crack propagation as layer-bridging areas of crack branching, thus causing a channelling of cracks into the material.
- The fracture phenomena found are characteristic for the components subject to load at high frequency and are virtually unknown in the literature. They were therefore initially described on the basis of familiar micromorphologic details and purely from the perspective of their occurrence.
- In accordance with [14], fracture morphologies of a fatigue failure in the form of fatigue striations were found in the material subject to loading at high frequency.
- This suggests that the same mechanisms are operating in the formation of fatigue fracture morphologies at high frequencies as in loading at low frequency. High load speeds therefore exert no influence.

- The fracture surfaces of specimens subject to high-frequency loading nevertheless evince characteristic morphologies in the inter-fibre areas. However, these should probably not be assigned to the cyclic component but to the dynamic load at high frequency.
- In future, it would therefore be possible to assign fracture surfaces to dynamic or dynamic-fatigue loading on the basis of their specific morphologies.
- Additional intensive investigations into the failure of CFRP under dynamic and dynamic-fatigue loading remain to be carried out.
- Intensive research and discussions are still required in order to investigate the causes of the failure and the mechanisms operating. Particular attention needs to be devoted to the formation of fracture morphologies.

ACKNOWLEDGEMENTS

One of us, K. Friedrich, expresses his thanks to the NATO Research and Technology Agency for the support of his cooperation with Greece on the subject of composites for crash absorber elements (G108).

References

1. **Reifsnider, K.L.** (ed.), "Fatigue of Composite Materials", Amsterdam, The Netherlands: Elsevier Science Publishers B.V., 1991
2. **Harris, B.** (ed.), "Fatigue in Composites", Cambridge, England: Woodhead Publishing Ltd., 2003
3. **Schulte K.**, "Faserverbundwerkstoffe mit Polymermatrix - Aufbau und mechanische Eigenschaften DLR 92-28", Forschungsbericht, Köln: DLR, 1992
4. **Sun, T.S.** and **Chan, W.S.**, "Frequency Effect on the Fatigue Life of a Laminated Composite", In: *Composite Materials: Testing and Design (Fifth Conference), ASTM STP 647*, Ed. S.W. Tsai, American Society for Testing and Materials, 1979, 418 - 430
5. **Friedrich, K.** (ed.), , "Application of Fracture Mechanics to Composite Materials", Amsterdam, The Netherlands: Elsevier Science Publishers B.V., 1989
6. **ESDU** Engineering Science Data Unit: "Endurance of Fibre-Reinforced Composite, Laminated Structural Elements Subjected to Simulated Random Acoustic Loading ESDU 84027". In: *ESDU Series on Vibration and Acoustic Fatigue*, London: ESDU International plc., 2001
7. **Holehouse, I.**, "Sonic Fatigue Design Techniques for Advanced Composite Airplane Structures", Thesis (Ph.D.), Southampton: University of Southampton, 1984
8. **Roylance, M.E.** and **Houghton, W.W.** and **Foley, G.E.**, "Characterisation of Cumulative Damage in Composites During Service" In: *Characterization, Analysis and Significance of Defects in Composite Materials AGARD – CP – 355*, 1983
9. **Wolf, N.D.** and **Jacobson, M.J.**, "Design and Sonic Fatigue Characteristics of Composite Material Components" In: *Symposium on acoustic fatigue, AGARD – CP – 113*, September 1972
10. **Friedrich, K.** and **Carlsson, L.A.** and **Gillespie, J.W. Jr.** and **Karger-Kocsis, J.**, "Fracture of Thermoplastic Composites" In: *Thermoplastic Composite Materials*, Ed. L.A. Carlsson. Amsterdam: Elsevier, 1991
11. **Purslow, D.**, "Matrix Fractography of Fibre Reinforced Epoxy Composites", *J. of Material Science*, **24** (1989), 176 – 172
12. **Hiley, M.J.**, "Fractographic Study of Static and Fatigue Failures in Polymer Composites", *Plastics, Rubber and Composites*, **28** 5 (1999), 210 – 227
13. **Heutling, F.** and **Franz, H.E.** and **Friedrich, K.**, "Mikrofraktographische Analyse des Delaminationswachstums in zyklisch belasteten Kohlenstofffaser / Duroplastharz – Verbundwerkstoffen", *Mat.-wiss. und Werkstofftechnik*, **29** (1998), 239 – 253
14. **Franz, H.E.**, "Beitrag zu Schwingbruchmorphologien in faserverstärkten Kunststoffen", *Mat.-wiss. u. Werkstofftech.*, **22** (1991), 435 – 444
15. **Symons D.D.** and **Davis G.**, "Fatigue Testing of Impact Damaged T300/914 Carbon-Fibre-Reinforced Plastic", *Composite Science and Technology*, **60** (2000), 379 – 389